EVIDENCE FOR A COSMOLOGICAL STRÖMGREN SURFACE AND FOR SIGNIFICANT NEUTRAL HYDROGEN SURROUNDING THE QUASAR SDSS J1030+0524

ANDREI MESINGER, ZOLTÁN HAIMAN

Department of Astronomy, Columbia University, 550 West 120th Street, New York, NY 10027

Accepted by ApJ Letters

ABSTRACT

A bright quasar residing in a dense and largely neutral intergalactic medium (IGM) at high redshifts ($z \gtrsim 6$) will be surrounded by a large cosmological Strömgren sphere. The quasar's spectrum will then show a sharp increase in resonant Lyman line absorption at wavelengths approaching and shorter than that corresponding to the Strömgren sphere's boundary along the line of sight. We show here that simultaneously considering the measured absorption in two or more hydrogen Lyman lines can provide the dynamical range required to detect this feature. We model broad and robust features of the Lyman α and Lyman β regions of the spectrum of the $z = 6.28$ quasar SDSS J1030+0524, using a hydrodynamical simulation. From the steep wavelength–dependence of the inferred absorption opacity, we detect the boundary of the Strömgren sphere at a proper distance of 6.0 ± 0.2 Mpc away from the source redshift. From the spectrum alone, we also find that beyond this distance, cosmic hydrogen turns nearly neutral, with a neutral fraction of $x_{\rm HI} \gtrsim 0.2$, and that the ionizing luminosity of this quasar is in the range $(5.2 \pm 2.5) \times 10^{56}$ photons sec^{-1}. The method presented here, when applied to future quasars, can probe the complex topology of overlapping ionized regions, and can be used to study the details of the reionization process.

Subject headings: cosmology: theory – cosmology: early universe – galaxies: formation – galaxies: high-redshift – galaxies: quasars: general – galaxies: quasars: absorption lines

arXiv:astro-ph/0406188v2 12 Jul 2004

1. INTRODUCTION

The ionization state of the IGM at redshift $6 \lesssim z \lesssim 7$ has been a subject of intense study over the past few years. While studies of the cosmic microwave background anisotropies by the *Wilkinson Microwave Anisotropy Probe (WMAP)* satellite imply that the IGM is significantly ionized out to $z \sim 15$, several pieces of evidence suggest that it has a large neutral fraction at $z \sim 6-7$ (see, e.g., Haiman 2003 for a recent review). If indeed the intergalactic hydrogen is largely neutral at $z \sim 6$, then quasars at this redshift should be surrounded by large ionized (HII) regions (Madau & Rees 2000; Cen & Haiman 2000). The imprint on the absorption spectrum of the damping wing of absorption by neutral hydrogen outside the HII region (Mesinger et al. 2004), and the size of the HII region itself (Wyithe & Loeb 2004) can be used to place stringent limits on the neutral fraction of the ambient IGM.

In principle, the quasar's absorption spectrum contains a record of the neutral fraction as a function of position along the line of sight. In Figure 1 we illustrate a model for the optical depth to Lyman α absorption as a function of wavelength towards a $z_Q = 6.28$ quasar embedded in a neutral medium ($x_{\rm HI} = 1$), but surrounded by a Strömgren sphere with a comoving radius of $R_S = 44$ Mpc. Around bright quasars, such as those recently discovered (Fan et al. 2001, 2003) at $z \sim 6$, the proper radius of such Strömgren spheres is expected to be $R_S \approx 7.7$ $x_{\rm HI}^{-1/3}$ ($\dot{N}_Q/6.5 \times 10^{57}$ s^{-1})$^{1/3}$ ($t_Q/2 \times 10^7$ yr)$^{1/3}$ $[(1+z_Q)/7.28]^{-1}$ Mpc (Madau & Rees 2000; Cen & Haiman 2000). Here $x_{\rm HI}$ is the volume averaged neutral fraction of hydrogen outside the Strömgren sphere and $\dot{N}_Q$, t_Q, and z_Q are the quasar's production rate of ionizing photons, age, and redshift. The fiducial values are those estimated for J1030+0524 (Haiman & Cen 2002; Wyithe & Loeb 2004). The mock spectrum shown in Figure 1 was created by computing the Lyman α opacity from a hydrodynamical simulation (the procedure is described in § 2 below). The optical depth at a given observed wavelength, $\lambda_{\rm obs}$, can be written as the sum of contributions from inside (τ_R) and out-

side (τ_D) the Strömgren sphere, $\tau_{\rm Ly\alpha} = \tau_R + \tau_D$. The residual neutral hydrogen inside the Strömgren sphere at redshift $z < z_Q$ resonantly attenuates the quasar's flux at wavelengths around $\lambda_\alpha(1+z)$, where $\lambda_\alpha = 1215.67$ Å is the rest-frame wavelength of the Lyman α line center. As a result, τ_R is a fluctuating function of wavelength (solid curve), reflecting the density fluctuations in the surrounding gas. In contrast, the damping wing of the absorption, τ_D, is a smooth function (dashed curve), because its value is averaged over many density fluctuations. As the figure shows, the damping wing of the absorption from the neutral universe extends into wavelengths $\lambda_{\rm obs} \gtrsim 8720$ Å, and can add significantly to the total optical depth in this region.

The sharp rise in τ_D at wavelengths $\lambda_{\rm obs} \lesssim 8720$ Å is a unique feature of the boundary of the HII region, and corresponds to absorption of photons redshifting into resonance outside of the Strömgren sphere. The detection of this feature has been regarded as challenging: since the quasar's flux is attenuated by a factor of $\exp(-\tau_{\rm Ly\alpha})$, an exceedingly large dynamical range is required in the corresponding flux measurements. *However, we show here that simultaneously considering the measured absorption in two or more hydrogen Lyman lines can provide the dynamical range required to detect this feature.* In particular, we model broad features of the Lyman α and Lyman β regions of the absorption spectrum of the $z = 6.28$ quasar SDSS J1030+0524. We find robust evidence for the boundary of the Stömgren sphere, and derive new limits on the neutral fraction of the ambient IGM, and on the ionizing emissivity of the quasar.[1]
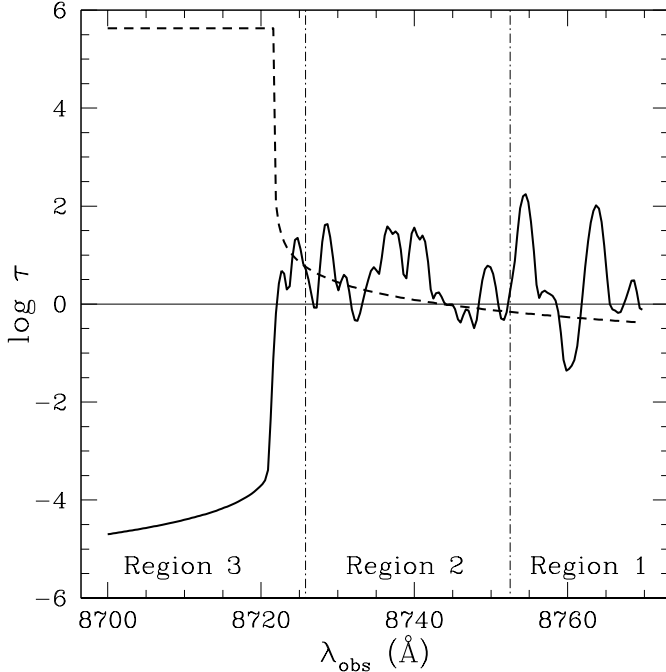
FIG. 1.— Model from a hydrodynamical simulation for the optical depth contributions from within (τ_R) and from outside (τ_D) the local ionized region for a typical line of sight towards a $z_Q = 6.28$ quasar embedded in a fully neutral, smooth IGM, with $R_S = 44$ Mpc and $f_{\rm ion} = 1$. The *dashed curve* corresponds to τ_D, and the *solid curve* corresponds to τ_R. The total Lyman α optical depth is the sum of these two contributions, $\tau_{\rm Ly\alpha} = \tau_R + \tau_D$. The *dashed-dotted lines* demarcate the three wavelength regions used for our analysis described in the text. In our analysis, the optical depths are averaged over 3.5 Å wavelength bins, which decreases the fluctuation of τ_R. For reference, the redshifted Lyman α wavelength is at 8852 Å, far to the right off the plot.

2. ANALYSIS

The observational input to our analysis is the deepest available absorption spectrum of SDSS J1030+0524 (White et al. 2003). The flux detection threshold in the Lyman α and Lyman β regions of this spectrum correspond to Lyman α optical depths of $\tau_{\rm lim(Ly\alpha)} \approx 6.3$ and $\tau_{\rm lim(Ly\beta)} \approx 22.8$ respectively.[2] The ratio of these two numbers is smaller than that of $(f_\alpha \lambda_\alpha)/(f_\beta \lambda_\beta)$, where f is the oscillator strength, mainly because of the need to subtract foreground Lyman α absorption in the Lyman β region. The Keck ESI spectrum of SDSS J1030+0524 exhibits a strong Lyman α Gunn-Peterson (GP) trough, with no detectable flux between wavelengths corresponding to redshifts $5.97 < z < 6.20$, as well as a somewhat narrower Lyman β trough between $5.97 < z < 6.18$ (White et al. 2003).

To summarize these constraints, we have divided the spectrum into three regions, shown in Figure 1. In Region 1, with $\lambda_{\rm obs} \geq 8752.5$ Å, the detection of flux corresponds to the *upper* limit on the optical depth $\tau_{\rm Ly\alpha} < 6.3$. Region 2, extending from 8725.8 Å $\leq \lambda_{\rm obs} < 8752.5$ Å, is inside the Lyman α trough, but outside the Lyman β trough. Throughout this region, the data requires $6.3 \lesssim \tau_{\rm Ly\alpha} \lesssim 22.8$. Region 3, with $\lambda_{\rm obs} < 8725.8$ Å has a *lower* limit $\tau_{\rm Ly\alpha} \geq 22.8$. As defined, each of these three regions contains approximately eight pixels.

---

[2] For our purposes, these optical depths can be taken as rough estimates. Their precise values are difficult to calculate, with $\tau_{\rm lim(Ly\beta)}$ especially uncertain (Songaila 2004; Lidz et al. 2002; Cen & McDonald 2002; Fan et al. 2002). However, we have verified that our conclusions below remain unchanged when the threshold opacities are varied well in excess of these uncertainties. In particular, considering ranges as wide as $5.5 < \tau_{\rm lim(Ly\alpha)} < 7$ and $10 < \tau_{\rm lim(Ly\beta)} < 30$ would lead to constraints similar to those we derive below.

We modeled the absorption spectrum, attempting to match these gross observed features. We do not perform a far more demanding pixel–by–pixel fit to the data, given the relatively poor quality of the spectra currently available. We utilized a hydrodynamical simulation that describes the density distribution surrounding the source quasar at $z = 6.28$. The details of the simulation are described elsewhere (Cen 2004, in preparation; Mesinger et al. 2004). We extracted density and velocity information from 100 randomly chosen lines of sight (LOSs) through the simulation box.[3] Along each line of sight (LOS), we computed the Lyman α absorption as a function of wavelength. The size of the ionized region (R_S) and the fraction of neutral hydrogen outside it ($x_{\rm HI}$) were free parameters. In addition, the quasar's ionizing luminosity, L_ν, was a third free parameter, $f_{\rm ion}$, defined by $L_\nu \equiv f_{\rm ion} L_\nu^e$. Here $L_\nu^e = 1.55 \times 10^{31}$ $(\nu/\nu_H)^{-1.8} [(1+z)/(1+z_Q)]^{-0.8}$, $\nu_H = 3.29 \times 10^{15}$ Hz is the ionization frequency of hydrogen, and z_Q is the source redshift ($z_Q = 6.28$ for SDSS J1030+0524). L_ν^e results from redshifting a power–law spectrum with a slope of $\nu^{-1.8}$, normalized such that the emission rate of ionizing photons per second is 1.3×10^{57}, matching the emissivity one obtains (Haiman & Cen 2002) for SDSS J1030+0524 using a standard template spectrum (Elvis et al. 1994). This translates to an emission rate of ionizing photons of $\dot{N}_Q \approx f_{\rm ion} \times 1.3 \times 10^{57}$ s^{-1}. To understand the significance of these parameters, note that changing R_S moves the dashed (τ_D) curve in Figure 1 left and right, while changing $x_{\rm HI}$ moves it up and down; changing $f_{\rm ion}$ moves the solid (τ_R) curve up and down. Values of $x_{\rm HI} < 1$ imply the existence of an ionizing background flux, with an ionization rate of $\Gamma_{12} \approx 10^{-5} x_{\rm HI}^{-1} \times 10^{-12}$ s^{-1}. We add this background flux to that of the quasar (the latter dropping as r^{-2} with distance), somewhat reducing the neutral hydrogen fraction inside the ionized region.

We evaluated τ_R and τ_D for each LOS, in the range of observed wavelengths 8700 Å $< \lambda_{\rm obs} <$ 8770 Å, and smoothed the optical depth by averaging $\exp(-\tau_{\rm Ly\alpha})$ over ~ 3.5 Å wavelength bins, corresponding to the Keck ESI spectral resolution of $R = 2500$ (White et al. 2003). This procedure was repeated for each combination of R_S, $x_{\rm HI}$, and $f_{\rm ion}$. We allowed $x_{\rm HI}$ to range from 1 to 10^{-3}, to trace its currently allowed range (Fan et al. 2002). Values of $R_S < 42$ Mpc (5.8 Mpc proper) are immediately ruled out by the presence of flux at $z \gtrsim 6.18$ in the redshifted Lyman β region of the spectrum. Hence, we let R_S range from 42 to 54 Mpc, in increments of 1 Mpc. Finally, $f_{\rm ion}$, was varied from 0.1 to 10, in increments of 0.1. For each point in the three–dimensional parameter space of R_S, $x_{\rm HI}$, and $f_{\rm ion}$, we computed the fraction of the 100 LOSs that were acceptable descriptions of the spectrum of SDSS J1030+0524, based on the criteria defined above. To be conservative, we allowed up to two pixels in each region to lie outside the allowed range of Lyman α optical depths; each LOS that had more than two pixels fail the above criteria in any of the three regions was rejected. We find that a more stringent criterion of allowing only a single 'faulty' pixel would strengthen our conclusions.

---

[3] The density and velocity distributions are biased near the density peaks where a quasar may reside. However, the spectral region of interest lies well outside these biased regions, which, in the case of high–redshift quasars, extends on average only to $\lesssim 1$ proper Mpc(Barkana & Loeb 2004). The use of randomly chosen LOSs is therefore an accurate statistical representation of the expected density and velocity fields.
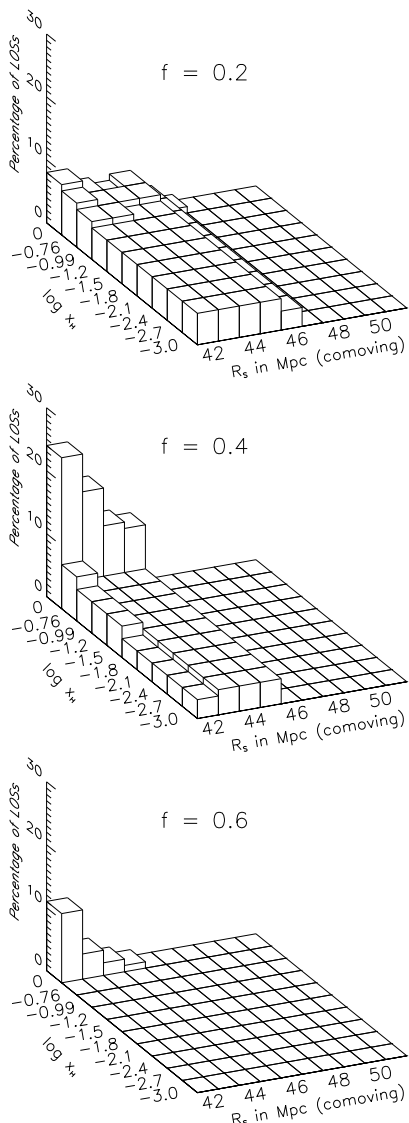
FIG. 2.— The percentages of LOSs that pass our analysis criteria. Results for three different values of the ionizing flux parameter, $f_{\rm ion}$ = 0.2, 0.4, 0.6 are shown in the *top*, *middle* and *bottom* panels, respectively. The fraction of accepted LOSs peaks sharply at a maximum of 24% at the parameter choice of $(R_S, x_{\rm HI}, f_{\rm ion})$ = (42 Mpc, 1, 0.4). The radius of the ionized region surrounding the quasar is limited to 42 Mpc $\leq R_S \leq$ 47 Mpc. The ionization flux parameter is tightly constrained around $f_{\rm ion}$ = 0.4, with no LOSs passing our criteria with values of $f_{\rm ion}$ < 0.2 and $f_{\rm ion}$ > 1.0. The peak at $x_{\rm HI}$ = 1 is over 3.4 times as likely as the next closest value of $x_{\rm HI}$ = 0.17, in which 7% of the LOSs pass.

3. RESULTS

The procedure outlined above turns out to provide tight constrains on all three of our free parameters *simultaneously*. The results are summarized in Figure 2, showing the percentage of LOSs that pass our analysis criteria, as a function of R_S, $x_{\rm HI}$, and $f_{\rm ion}$. The fraction of accepted LOSs peaks sharply at a maximum of 24% at the parameter choice of $(R_S, x_{\rm HI}, f_{\rm ion})$ = (42 Mpc, 1, 0.4). The radius of the ionized sphere is limited to 42 Mpc $\leq R_S \leq$ 47 Mpc, with no LOSs passing our criteria outside of that range. Note that an offset in the Lyman α line center by ± 1000 km s^{-1} (typical of quasar jets, for example), would represent an additional ± 1.5 Mpc uncertainty on the inferred radius. Although SDSS J1030+0524 has a precise redshift determination from C IV and N V lines, a

redshift error of $\Delta z = 0.01 - 0.02$ (typical in the absence of such metal lines) would add an uncertainty of $\pm (4 - 8)$ Mpc to any analysis similar to the one presented here. The ionization flux parameter is tightly constrained around $f_{\rm ion} = 0.4$, with no LOSs passing our criteria with values of $f_{\rm ion} < 0.2$ and $f_{\rm ion} > 1.0$. The peak value of $f_{\rm ion} = 0.4$ implies an emission rate of $(5.2 \pm 2.5) \times 10^{56}$ photons sec^{-1}. Finally, the peak at $x_{\rm HI} = 1$ is over 3.4 times as likely as the next closest value of $x_{\rm HI} = 0.17$, in which 7% of the LOSs pass, and 6 times as likely as values of $x_{\rm HI} < 0.016$, in which 4% of the LOSs pass.

These results can be interpreted as follows. As mentioned previously, the presence of flux in Region 2 ($\tau_{\rm Ly\alpha} < 22.8$) sets a *lower limit* on R_S, implying that the edge of the ionized region must be at a smaller wavelength than the boundary between Regions 2 and 3. Region 3, however, yields an *upper limit* on R_S, from the requirement that $\tau_{\rm Ly\alpha} > 22.8$ in that region. This high optical depth cannot be maintained by τ_R alone, without violating the constraint in Region 1 of $\tau_{\rm Ly\alpha} < 6.3$. We emphasize that the *upper limit* on R_S makes no use of the data in Region 2. Hence the edge of the ionized region must be close to the boundary between Regions 2 and 3. The ionization flux is constrained due to our criteria in Regions 1 and 2. An ionization flux that is too small (*large* τ_R) would violate $\tau_{\rm Ly\alpha} < 6.3$ in Region 1. An ionization flux that is too large (*small* τ_R) would violate $\tau_{\rm Ly\alpha} > 6.3$ throughout Region 2, since the damping wing contribution to $\tau_{\rm Ly\alpha}$ is insufficient, given the lower limit on R_S above. Our constraint on the neutral hydrogen fraction, $x_{\rm HI}$, comes from the presence of flux in the Lyman β region of the spectrum corresponding to Region 2. Because of fluctuations in the density field (and hence in τ_R), a strong damping wing is needed to raise $\tau_{\rm Ly\alpha}$ above 6.3 throughout Region 2, *while still preserving $\tau_{\rm Ly\alpha} < 6.3$ in Region 1.*

4. DISCUSSION AND CONCLUSIONS

Using only the lower limits on the Lyman α optical depth obtained from the Lyman α and Lyman β GP troughs of SDSS J1030+0524, we find a simultaneous constraint on the size of the ionized region surrounding this quasar, the neutral fraction of the ambient intergalactic medium, and the ionizing luminosity of the quasar.

The radius of the Strömgren sphere is limited to 42 Mpc $\leq R_S \leq 47$ Mpc, close to the previously estimated lower limits (Madau & Rees 2000; Cen & Haiman 2000). We also find evidence that the IGM was significantly neutral at $z \sim 6$, with a $\sim 1\,\sigma$ lower limit of $x_{\rm HI} \gtrsim 0.17$. This result is derived from the observed sharpness of the boundary of the HII region alone, and relies only on the gross density fluctuation statistics from the numerical simulation. In particular, it does not rely on assumptions about the mechanism for the growth of the HII region. Our results provide a robust confirmation of previous suggestions that the IGM was significantly more neutral at $z \sim 6$ than the lower limit of $x_{\rm HI} \gtrsim 10^{-3}$ that is directly obtainable from the black region (Gunn–Peterson trough) of the quasar spectra. Finally, we find an emission rate of ionizing photons per second of $(5.2 \pm 2.5) \times 10^{56}$ photons sec^{-1}, which is between 2 – 10 times lower than expected (Elvis et al. 1994; Telfer et al. 2002), strengthening arguments that reionization at $z \sim 6$ is caused by the radiation from early stars, rather than bright quasars (e.g. Dijkstra et al. 2004).

Our findings represent the first detection of the boundary of a cosmological HII region, and have several important implications. It has recently been shown that tight constraints on

the hydrogen neutral fraction can be extracted directly from the Lyman α absorption spectrum alone (Mesinger et al. 2004), but this requires tens of spectra to be statistically significant when R_S is not known. Incorporating an independent limit on R_S, such as the one obtained from this method, can reduce the number of required spectra to *one*. Tight constraints on x_{HI} have also recently been obtained by adopting a proper size of $R_S \approx 4.5$ Mpc for SDSS J1030+0524, together with an estimate of its lifetime (Wyithe & Loeb 2004). Our direct determination of the Strömgren sphere size is only slightly larger than the previously adopted value, lending further credibility to this conclusion.

The sharp boundary we detect also constrains the hardness of the ionizing spectrum of SDSS J1030+0524. We infer here a rise in the neutral fraction over a redshift interval of $\Delta z \sim 0.02$, corresponding to a proper distance of ~ 1.2 Mpc. In order for its mean free path not to significantly exceed this thickness, the energy of the typical ionizing photon emitted by SDSS J1030+0524 must be < 230eV. This implies that the effective slope of the ionizing spectrum of this source is softer than $-d \ln L_\nu / d \ln \nu = 1.07$. This analysis ignores radiative transfer effects, which can further blur the apparent boundary of the HII region, and would strengthen this limit.

The analysis presented here uses only the Lyman β and Lyman α absorption spectra for the single quasar J1030+0524, but can be extended by incorporating additional Lyman lines, which provide further constraints on the optical depth. Although such analysis will have additional uncertainties associated with the need to subtract foreground absorption due to the lower Lyman transitions, it is likely that adding the Lyman γ line can tighten the constraints obtained here (Fan et al. 2002). Note that the presence of dust within the HII region can attenuate and redden the observed spectrum. This will not, however, impact our conclusions, since the overall attenuation is absorbed into f_{ion}, and reddening extends over a wavelength range much broader than the sharp features considered here.

In the future, given a larger sample of quasars (and/or a sample of gamma–ray burst afterglows with near-IR spectra) at $z > 6$, it will be possible to use the method presented here to search for sharp features in the absorption spectrum from intervening HII regions, not associated with the background source itself. We plan study the utility of this approach in a future paper. For such external HII regions that happen to intersect the line of sight, both the red and the blue sides of each GP trough can, in principle, be detected, and can yield two separate measurements of the ionized fraction at different points along the line of sight. The Universe must have gone through a transition epoch when HII regions, driven into the IGM by quasars and galaxies, partially percolated and filled a significant fraction of the volume. The detection of the associated sharp features in future quasar absorption spectra will provide a direct probe of the the 3D topology of ionized regions during this crucial transition epoch. Deep surveys equipped with sufficiently red filters (with instruments such as those being carried out by the VLT, and ultimately with deep surveys covering a significant portion of the sky, such as the survey proposed with the Large-aperture Synoptic Survey Telescope, LSST; Tyson (2002)) will be able to deliver a large sample of bright $z > 6$ quasars needed for such studies.

REFERENCES

Barkana, R., & Loeb, A. 2004, ApJ, 601, 64
Becker, R. H., et al. 2001, AJ, 122, 2850
Cen, R. 2003, ApJ, 591, L5
Cen, R., Haiman, Z., & Mesinger, A. 2004, ApJ, submitted, astro-ph/0403419
Cen, R., & Haiman, Z. 2000, ApJ, 542, L75
Cen, R., & McDonald, P. 2002, ApJ, 570, 457
Dijkstra, M., Haiman, Z., & Loeb, A. 2004, ApJ, in press, astro-ph/0403078
Elvis, M., et. al. 1994, ApJS, 95, 1
Fan, X., et al. 2001, AJ, 122, 2833
Fan, X., et al. 2002, AJ, 123, 1247
Fan, X., et al. 2003, AJ, 125, 1649
Haiman, Z. 2003, to appear in Carnegie Observatories Astrophysics Series, Vol. 1: Coevolution of Black Holes and Galaxies, ed. L. C. Ho (Cambridge: Cambridge Univ. Press); astro-ph/0304131
Haiman, Z., Abel, T., & Madau, P. 2001, ApJ, 551, 599
Haiman, Z., & Cen, R. 2002, ApJ, 578, 702
Haiman, Z. & Holder, G. P. 2003, ApJ, 595, 1
Lidz, A., Hui, L., Zaldarriaga, M., & Scoccimarro, R. 2002, ApJ, 579, 491
Madau, P., & Rees, M. J. 2000, ApJ, 542, L69
Mesinger, A., Haiman, Z., & Cen, R. 2004, ApJ, in press, astro-ph/0401130
Shapiro, P. R., Giroux, M. L., & Babul, A. 1994, ApJ, 427, 25
Songaila, A. 2004, AJ, 127, 2598
Songaila, A., & Cowie, L. L. 2002, AJ, 123, 2183
Spergel, D.N. et al. 2003, AJS, 148, 175
Telfer, R. C., Zheng, W., Kriss, G. A. 2002, AJ, 565, 773
Tyson, J. A. 2002, Proc. SPIE Int. Soc. Opt. Eng., 4836, 10
White, R. L., Becker, R. H., Fan, X., & Strauss, M. A. 2003, AJ, 126, 1
Wyithe, J. S. B. & Loeb, A. 2003, ApJL, 588, L69
Wyithe, J. S. B., & Loeb, A. 2004, Nature, 427, 815